Precooling Strategy Allows Exponentially Faster Heating

A. Gal and O. Raz
Department of Physics of Complex Systems, Weizmann Institute of Science, 76100 Rehovot, Israel

(Received 16 May 2019; revised manuscript received 26 November 2019; accepted 22 January 2020; published 13 February 2020)

What is the fastest way to heat a system which is coupled to a temperature controlled oven? The intuitive answer is to use only the hottest temperature available. However, we show that often it is possible to achieve an exponentially faster heating protocol. Surprisingly, this protocol can have a precooling stage—cooling the system before heating it shortens the heating time significantly. To demonstrate such improvements in many-body systems, we developed a projection-based method with which such protocols can be found in large systems, as we demonstrate on the 2D antiferromagnet Ising model.

DOI: 10.1103/PhysRevLett.124.060602

Consider the common task of cooling a hot system by coupling it to a thermal reservoir with a controlled temperature, as a refrigerator. It is counterintuitive but well understood that a preceding heating stage followed by a slow cooling stage often shortens the overall cooling time. Indeed, *annealing* techniques are widely used in the industrial treatment of metals, glasses, and crystal lattices [1,2]. A similar approach is used in simulated annealing [3–6]. These Monte Carlo (MC) optimization algorithms find an approximation of the global minimum of a function, using an artificial temperature which characterizes the probability to accept a step to a state with a different value of this function. In order to escape local minima, the temperature is initially set to a high value, then slowly decreased. Another nonmonotonic relaxation phenomenon is the Mpemba effect (ME) [7–13], where an initially hot system cools faster than an identical system initiated at a lower temperature. In contrast to annealing, where the heating can be fast but the cooling must be slow, in the ME the temperature of the bath is lowered instantaneously. Although the ME seems to suggest that a preheating stage can shorten cooling processes, it is not necessarily the case since the preceding stage might take a longer time than gained.

Are there cases where it is faster to heat a system by first cooling it? Improving the heating rate by changing other variables was already concerned in the shortcut to adiabaticity literature [14–16] and is relevant in many applications. For example, shortening the heating stroke period in a heat engine can improve its power output [15,17,18]. The recently introduced inverse Mpemba effect (IME) [19], where a cold system heats faster than an identical system initiated at a warmer temperature, suggests that this might be possible. Nevertheless, it does not imply that precooling speeds up heating for a similar reasoning as in the ME—the cooling stage might take a longer time than gained by the IME.

In this manuscript we show that a precooling strategy can result in an exponentially faster heating. After formulating the problem of optimal heating, we find the optimal heating protocol in a four-state system, and a simple precooling protocol in a diffusion problem. In both examples the system does not exhibit any variant of the IME, demonstrating that such protocols are not a consequence of the IME, and are expected in a wider range of systems. To address many-body systems and avoid intractable calculations, we then extend our strategy by a projection of the dynamics into a lower dimension space. This method is demonstrated in the 2D antiferromagnet Ising model.

To define "shorter heating time," we next introduce the mathematical setup. For simplicity let us first consider systems with N states. Let $p_i(t)$ denote the probability to find the system in state i at time t. A probability distribution of an N-state system is represented by $\mathbf{p} = (p_1, \ldots, p_N)$, with $\sum_{i=1}^{N} p_i = 1$. The thermal bath is assumed to have zero memory, and thus the dynamic of $\mathbf{p}(t)$ is Markovian,

$$\dot{\mathbf{p}}(t) = R(T_b)\mathbf{p}(t). \tag{1}$$

The transition rate from state j to state i is given by the matrix element $R_{ij}(T_b)$ where T_b is the bath temperature. A diagonal element $R_{ii}(T_b) = -\sum_{j\neq i} R_{ji}(T_b)$ is the minus of the escape rate from state i. As $R(T_b)$ describes relaxation towards equilibrium, it is detailed balanced and its equilibrium probability distribution, denoted by $\boldsymbol{\pi}(T_b)$, is given by the Boltzmann distribution:

$$\pi_i(T_b) = \frac{1}{\mathcal{Z}} e^{-E_i/T_b}, \qquad \mathcal{Z} = \sum_i e^{-E_i/T_b}, \tag{2}$$

where E_i is the energy of state i and T_b is in units where $k_B = 1$. By writing $R(T_b)$ we assume that the only degree of control at our disposal is the bath temperature.

We consider heating processes in which the system is initiated at the equilibrium $\boldsymbol{\pi}(T_0)$ for a specific temperature $T_0 < T_{\max}$, where $T_{\max}$ is the maximal temperature of the bath. Our goal is to heat the system towards the hot equilibrium $\boldsymbol{\pi}(T_{\max})$. The dynamic is defined by the heating protocol $T_b(t)$—bath temperature as a function of time—limited by $T_b(t) \leq T_{\max}$. The trajectory in the probability space generated by $T_b(t)$ is

$$\mathbf{p}(t) = \mathcal{T}\{e^{\int_0^t R(T_b(t'))dt'}\}\boldsymbol{\pi}(T_0), \tag{3}$$

where $\mathcal{T}$ is the time-ordering operator [20].

In what follows we consider protocols that during the time interval $t \in [0, \tau]$ are constrained by $T_b(t) \leq T_{\max}$, and for $t > \tau$ the bath temperature is set to $T_{\max}$. These are compared to the *oven* protocol, where $T_b(t) = T_{\max}$ at all times.

To gain some insight, it is beneficial to decompose $\mathbf{p}(t)$ in terms of the right eigenvectors of $R(T_{\max})$. Let $\mathbf{v}_i \equiv \mathbf{v}_i(T_{\max})$ be a solution of

$$R(T_{\max})\mathbf{v}_i = \lambda_i \mathbf{v}_i, \tag{4}$$

where $0 = \lambda_1 > \lambda_2 \geq \lambda_3 \geq \cdots \geq \lambda_N$ are the eigenvalues of $R(T_{\max})$, which are real valued as $R(T_{\max})$ is detailed balanced [21]. $\mathbf{p}(t)$ can be expressed as

$$\mathbf{p}(t) = \boldsymbol{\pi}(T_{\max}) + \sum_{i=2}^{N} a_i(t)\mathbf{v}_i. \tag{5}$$

For $t > \tau$, the rate matrix is fixed since $T_b(t) = T_{\max}$, and the dynamic is simplified to

$$a_i(t) = a_i(\tau)e^{\lambda_i(t-\tau)}, \tag{6}$$

where $a_i(\tau)$ are determined by the protocol $T_b(t)$. For the oven protocol, the dynamic is even simpler,

$$a_i(t) = a_i(0)e^{\lambda_i t}, \tag{7}$$

where $a_i(0) \equiv a_i^{T_0}$ is the coefficient of $\mathbf{v}_i$ in $\boldsymbol{\pi}(T_0)$.

Following Eqs. (5) and (6), we suggest to minimize the magnitudes of $a_i(\tau)$ by their order. The exponential time dependence in Eq. (6) implies that at long enough time the dominant component in Eq. (5) is the slowest one. Consequently, $a_2(t)$ dominates the distance to equilibrium, regardless of the values of $a_i(\tau)$ for $i > 2$. Therefore, the optimal protocol is the one that minimizes $|a_2(\tau)|$. If there are several protocols with $a_2(\tau) = 0$, then among these we should choose the protocol that minimizes $|a_3(\tau)|$, and so on. The optimal protocol thus sets $0 = a_2(\tau) = a_3(\tau) = \cdots = a_m(\tau)$ for the largest m possible and minimizes $|a_{m+1}(\tau)|$. In the Supplemental Material (SM) [22] we show a generalization of the above to nonlinear dynamics.

To demonstrate the construction of the optimal heating protocol, we consider a simple example of a four-state system. The temperature dependence of R is of Arrhenius form,

$$R_{ij}(T_b) = \Gamma e^{-(B_{ij}-E_j)/T_b} \quad (i \neq j), \tag{8}$$

where Γ is the rate constant, $B_{ij} = B_{ji}$ are the barriers between states i and j, and E_i is the energy of state i. Specifically, we use $E_i = (0, 0.4, 1, 0.2)$, and $B_{12} = 1.5$, $B_{13} = 1.1$, $B_{23} = 10$, $B_{24} = 0.01$, $B_{34} = 1$, and $B_{14} = \infty$ as there is no direct transition between states 1 and 4. The maximal temperature is set to $T_{\max} = 2$, and the initial temperature to $T_0 = 1$.

To find the optimal heating protocol, we follow the above strategy—minimizing $|a_i(\tau)|$ by their order. We first minimize $|a_2(\tau)|$, or equivalently $[a_2(\tau)]^2$, for $\tau = 1$, and find many protocols with $a_2(\tau) = 0$. Next, we minimize $[a_3(\tau)]^2$ keeping $a_2(\tau) = 0$, and find many protocols where both $a_2(\tau) = 0$ and $a_3(\tau) = 0$. However, it is impossible to set $a_2(\tau) = a_3(\tau) = a_4(\tau) = 0$, which corresponds to $\mathbf{p}(\tau) = \boldsymbol{\pi}(T_{\max})$. Therefore, the optimal heating problem is

$$\underset{T_b(t)\leq T_{\max}, 0<t\leq\tau}{\operatorname{argmin}} [a_4(\tau)]^2, \quad \text{s.t.} \quad a_2(\tau) = a_3(\tau) = 0. \tag{9}$$

In the language of optimal control theory, this problem is a quadratic end-point minimization, with the dynamic in Eq. (1), linear end-point constraints, a bounded domain and no path cost. Such minimization problems can be addressed numerically using Pontryagin's maximum principle [23]. Since there is no path cost, it can also be solved numerically with methods as the sequential quadratic programming [24]. We use both the free OpenOCL package [25] which implements the Pontryagin's maximum principle, and the MATLAB built-in function *fmincon* which implement sequential quadratic programming, to solve this optimization problem, discretizing time into 400 points. The two methods converge to the same optimal protocol $T_b(t)$ plotted in Fig. 1(a). Surprisingly, it contains a precooling stage.

As shown in Fig. 1(b), a_2 at $\boldsymbol{\pi}(T)$, denoted by a_2^T, is monotonic with temperature, meaning that the system does not show any type of an IME. Nevertheless, heating can be improved by precooling, as can be seen in Fig. 1(c). In this figure, we compare the Kullback-Leibler (KL) divergence [19,26] of $\mathbf{p}(t)$ to $\boldsymbol{\pi}(T_{\max})$ in two protocols. In both the system is initiated at $\boldsymbol{\pi}(T_0)$, but evolves under different $T_b(t)$: (i) orange dashed line—the oven protocol, where $T(t) = T_{\max}$ at all times; (ii) green solid line—the optimal protocol plotted in Fig. 1(a). As illustrated, the optimal protocol achieves an exponentially faster relaxation towards equilibrium.

Finding the optimal heating protocol in systems with a high dimensional probability space is very tedious and

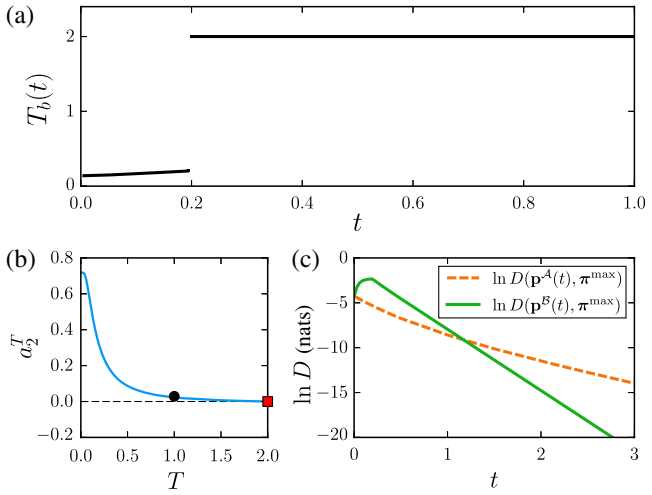

FIG. 1. Four-state system. (a) The optimal heating protocol $T_b(t)$. The precooling stage takes place in $0 \le t \lesssim 0.2$, where $T_b(t) < T_0 = 1$. For $t \gtrsim 0.2$ the bath temperature is fixed as $T_b(t) = T_{\max} = 2$. (b) The coefficient a_2^T of the slowest direction $\mathbf{v}_2$ in the equilibrium distribution $\boldsymbol{\pi}(T)$. The red square is at $T_{\max} = 2$ where $a_2 = 0$ and the black dot is at the initial temperature $T_0 = 1$. The coefficient a_2 is monotonic, therefore the system does not exhibit any type of IME. (c) The log distance (KL divergence) to the equilibrium $\boldsymbol{\pi}(T_{\max}) = \boldsymbol{\pi}^{\max}$ of the trajectories generated by the oven protocol ($\mathcal{A}$, dashed orange) and the optimal protocol ($\mathcal{B}$, solid green), both initiated at $\boldsymbol{\pi}(T_0)$.

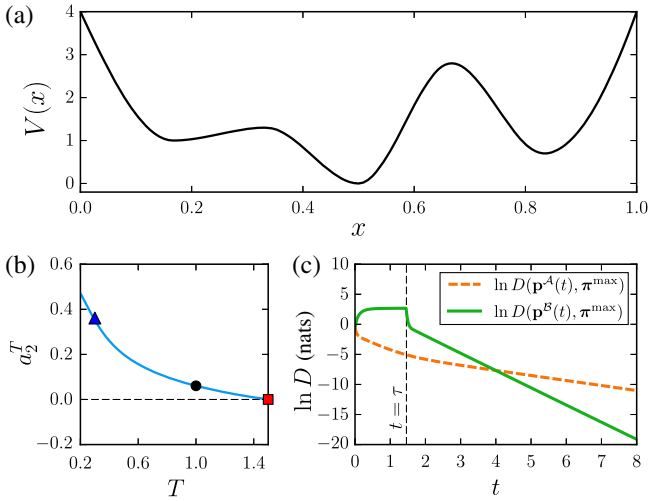

FIG. 2. A Brownian particle in a potential. (a) The potential $V(x)$. (b) The coefficient a_2^T as a function of T. The red square is at $T_{\max} = 1.5$ where $a_2 = 0$, the black dot is at the initial temperature $T_0 = 1$, and the blue triangle is at the cold temperature $T_{\text{cold}} = 0.3$. a_2^T is monotonic, therefore the system does not exhibit any type of IME. (c) The log-KL divergence to $\boldsymbol{\pi}(T_{\max}) = \boldsymbol{\pi}^{\max}$ of the trajectories generated by the oven protocol ($\mathcal{A}$, dashed orange) and the precooling protocol ($\mathcal{B}$, solid green), both initiated at $\boldsymbol{\pi}(T_0)$. The precooling duration is $\tau = 1.46$, after which the precooling protocol achieves exponentially faster relaxation towards equilibrium.

generally impractical. However, in some cases it is possible to improve the heating time exponentially by a short precooling stage with a fixed cold temperature. Let us demonstrate this through the following example: a Brownian particle diffusing in a 1D potential with reflecting boundary conditions, described by the Fokker-Planck equation

$$\dot{p}(x,t) = \frac{1}{\gamma}\partial_x[(\partial_x V(x))p(x,t)] + \frac{T_b}{\gamma}\partial_x^2 p(x,t), \qquad (10)$$

where $p(x,t) \equiv \mathbf{p}(t)$ is the probability distribution of finding the particle at position $x \in (0,1)$ at a given time t. For simplicity we assume that the damping coefficient is given by $\gamma = 1$.

For the potential $V(x)$ in Fig. 2(a) and a system initiated at $\boldsymbol{\pi}(T_0)$, we consider two protocols: (i) the oven protocol (orange dashed line); (ii) a precooling protocol (green solid line), where the system is first coupled to a T_{cold} bath for a finite duration τ, and then to the $T_{\max}$ bath. During the precooling stage the distance to $\boldsymbol{\pi}(T_{\max})$ increases while $a_2(t)$ decreases and vanishes at $t = \tau$. For $t > \tau$, the system relaxes exponentially faster towards its equilibrium, as can be seen from the different slopes of the log distance in Fig. 2(c). As in the previous example in Fig. 1, this system does not show any type of an IME, since a_2^T in Fig. 2(b) is monotonic with temperature [27].

Under what conditions can precooling improve heating? For systems that exhibit a strong inverse Mpemba effect (SIME), a simple argument for the existence of such a protocol can be given. The SIME is defined by the existence of a temperature $T_M < T_{\max}$ at which a_2^T changes its sign [29]. If this effect exists in the system, then the oven protocol is necessarily not optimal for any initial temperature $T_M < T_0 < T_{\max}$. Precooling the system to temperature $T_{\text{cold}} < T_M$ initiates a trajectory from $\boldsymbol{\pi}(T_0)$ towards $\boldsymbol{\pi}(T_{\text{cold}})$, where these two equilibrium points have a different sign of a_2^T. Therefore, the trajectory must cross the $a_2 = 0$ manifold at finite time. The SIME thus assures that a precooling protocol can be constructed to eliminate a_2 at a finite time and thereby improve the heating rate exponentially. Moreover, the SIME was shown to be both robust and to appear with a non-negligible probability [29], and therefore the same holds for precooling protocols in the presence of a SIME. An example that provides a physical intuition for this case is given in the SM [22].

In systems that do not show the SIME, a precooling protocol can still exist, although the previous discussion does not apply. Without a SIME, a_2^T has the same sign for any $T < T_{\max}$. Therefore, in any slow enough protocol $\mathbf{p}(t)$ does not cross the $a_2 = 0$ manifold. Therefore, in contrast to systems that show the SIME where the existence of a precooling protocol depends only on the location of $\boldsymbol{\pi}(T_{\text{cold}}) \equiv \mathbf{v}_1(T_{\text{cold}})$, in any other system it must depend

on some of the faster dynamics encoded in $\mathbf{v}_i(T_{\text{cold}})$ for $i \geq 2$. As generically the eigenvectors and their coefficients are continuous in the temperature, we expect the effect to exist in some range around T_{cold}.

In the analysis so far, the Markovian operator and its second eigenvector $\mathbf{v}_2$ played a crucial role. It is therefore rarely applicable to many-body systems, where the number of microstates grows exponentially with the number of particles and thus finding $\mathbf{v}_2$ or $\boldsymbol{\pi}(T_0)$ is a highly nontrivial task. To overcome this limitation, we next extend our strategy by considering a projection of the high-dimensional probability space trajectories into a lower dimension space.

Given a many-body system, we first choose two different observables, x_1 and x_2, that can be easily calculated for any microstate of the system. A probability distribution $\mathbf{p}$ can then be projected into a 2D space by the $\mathbf{p}$ averaging of x_1 and x_2 over all microstates, given by $(\langle x_1\rangle_{\mathbf{p}}, \langle x_2\rangle_{\mathbf{p}})$. Whereas it is impractical to follow the time evolution of $\mathbf{p}(t)$ in a system with a huge number of microstates, $\langle x_1\rangle_{\mathbf{p}(t)}$ and $\langle x_2\rangle_{\mathbf{p}(t)}$ can be evaluated to a high precision using a standard MC simulation. As discussed above, in the full probability space all trajectories $\mathbf{p}(t)$ asymptotically approach $\boldsymbol{\pi}(T_{\text{max}})$ from the slowest direction $\mathbf{v}_2$, except for ones that are on the fast manifold. Therefore, their projections $(\langle x_1\rangle_{\mathbf{p}(t)}, \langle x_2\rangle_{\mathbf{p}(t)})$ approach the mapped equilibrium $(\langle x_1\rangle_{\boldsymbol{\pi}(T_{\text{max}})}, \langle x_2\rangle_{\boldsymbol{\pi}(T_{\text{max}})})$ from the projection of $\mathbf{v}_2$ direction [30]. In contrast, trajectories on the fast manifold approach $\boldsymbol{\pi}(T_{\text{max}})$ from a different direction $\mathbf{v}_i$ $(i \geq 3)$, and projected to trajectories that approach the mapped equilibrium from the projection of the $\mathbf{v}_i$ direction [31].

Let us demonstrate the projection method in a concrete many-body system. We consider the 2D Ising model on a $L \times L$ square lattice, with external magnetic field, antiferromagnetic nearest neighbor interactions, and periodic boundary conditions. We denote the state of the spin located at the ith row and jth column by $\sigma_{ij} \in \{-1, 1\}$. The Hamiltonian of the system is given by

$$\mathcal{H} = -\frac{J}{4}\sum_{\langle ij,kl\rangle}\sigma_{ij}\sigma_{kl} - h\sum_{ij}\sigma_{ij}, \tag{11}$$

where $J = -1$ is the antiferromagnet coupling constant and h is the external magnetic field. The first summation is restricted to nearest neighbor spins, and the second summation is over all spins in the system. The dynamic is chosen to be the single spin flip Glauber dynamic [32]. The rate of flipping a spin is given by

$$R_{\text{flip}}(T_b) = \frac{1}{1 + e^{\Delta E/T_b}}, \tag{12}$$

where ΔE is the energy increment due to the flip.

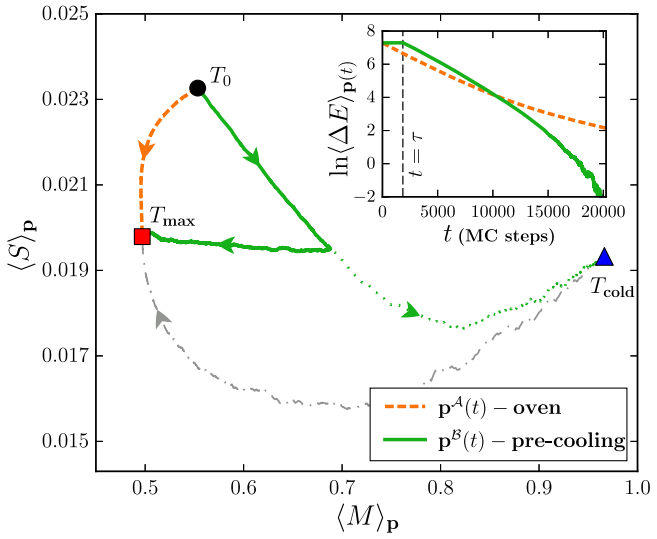

FIG. 3. 2D Ising model with external magnetic field $h = 1.0025$. The black dot, red square, and blue triangle are the mapped equilibrium points $(\langle M\rangle_{\boldsymbol{\pi}(T)}, \langle S\rangle_{\boldsymbol{\pi}(T)})$ at $T_0 = 0.125$, $T_{\text{max}} = 0.625$, and $T_{\text{cold}} = 0.0125$, respectively. The oven protocol trajectory (orange dashed line) is initiated at T_0 and approaches the T_{max} equilibrium from the projection of $\mathbf{v}_2$ direction. The trajectory initiated at T_{cold} (gray dot-dashed line) evolves under the oven protocol and approaches the same equilibrium from an opposite direction. The precooling protocol trajectory (green solid line), with a precooling duration of $\tau = 1850$ MC steps, approaches the T_{max} equilibrium from a different direction and thus from the fast manifold. The green dotted line is the trajectory the system would have followed had it stayed coupled to T_{cold}. Inset: the difference between the energy $\mathbf{p}$-averaging of a trajectory and equilibrium, plotted for the oven and precooling protocols.

As already mentioned, there is no hope to find $\mathbf{v}_2$ numerically, even for a moderate case of $L = 70$, corresponding to 2^{4900} microstates. To project $\mathbf{p}(t)$, we thus choose two observables: the mean and staggered magnetization, defined for a microstate by

$$M = L^{-2}\sum_{ij}\sigma_{ij}; \qquad S = L^{-2}\left|\sum_{ij}s(ij)\sigma_{ij}\right|, \tag{13}$$

where $s(ij) = 1$ (-1) for even (odd) value of $i + j$, specifying two sublattices, and the absolute value in S is used since the two sublattices are symmetric due to periodic boundary conditions.

Finding a precooling protocol in the 2D Ising model described above with $L = 70$ is demonstrated in Fig. 3. The projected trajectories $(\langle M\rangle_{\mathbf{p}(t)}, \langle S\rangle_{\mathbf{p}(t)})$ were calculated using 10^7 realizations of a MC simulation. To sample the realizations from $\boldsymbol{\pi}(T_0)$, the state of every spin in each realization was chosen randomly, and the Glauber dynamic was applied to all the realizations for 10^6 MC steps, with $T_b = T_0$ (for details, see SM [22]). After preparation,

the oven protocol, denoted by $\mathcal{A}$, was applied and $(\langle M\rangle_{\mathbf{p}^{\mathcal{A}}(t)}, \langle S\rangle_{\mathbf{p}^{\mathcal{A}}(t)})$ was measured. As Fig. 3 shows, another trajectory (gray dot-dashed line), where the system is prepared at $T_b = T_{\text{cold}}$ and evolves under the same protocol, approaches the same equilibrium point from the opposite direction. Namely, one of these trajectories approaches from the $\mathbf{v}_2$ direction and the other from $-\mathbf{v}_2$. This implies that the sign of a_2 at $\boldsymbol{\pi}(T_{\text{cold}})$ is opposite to that of $\boldsymbol{\pi}(T_0)$. If a trajectory approaches the equilibrium point from a different direction than the previous two, it must lie on the $a_2 = 0$ manifold, and thereby have an exponentially faster relaxation towards the equilibrium. The precooling protocol, denoted by $\mathcal{B}$, was found by choosing τ such that the corresponding trajectory $(\langle M\rangle_{\mathbf{p}^{\mathcal{B}}(t)}, \langle S\rangle_{\mathbf{p}^{\mathcal{B}}(t)})$ approaches the equilibrium point from a different direction.

To demonstrate that the precooling protocol is indeed faster, we used the $\mathbf{p}$-averaged energy difference to measure the distance of a trajectory to equilibrium, as suggested in [13]. This distance function captures the faster relaxation rate of the precooling protocol, compared to the oven protocol, as shown in the inset of Fig. 3.

We have demonstrated how heating processes in several systems can be exponentially improved using a precooling strategy. As we demonstrated, our method can be applied even in many-body systems, and is expected to be relevant to experiments as well.

O. R. is the incumbent of the Shlomo and Michla Tomarin career development chair, and is supported by the Abramson Family Center for Young Scientists and by the Israel Science Foundation, Grant No. 950/19. We would like to thank H. Aharoni, V. V. Prasad, O. Hirschberg, M. Vucelja, and I. Klich for useful discussions.

[1] J. L. Dossett and H. E. Boyer, *Practical Heat Treating* (ASM International, Materials Park, Ohio, 2006).
[2] F. J. Humphreys and M. Hatherly, *Recrystallization and Related Annealing Phenomena* (Elsevier, Oxford, 2012).
[3] S. Kirkpatrick, C. D. Gelatt, and M. P. Vecchi, Science **220**, 671 (1983).
[4] L. Ingber, J. Control Cybern. **25**, 33 (1996).
[5] J. De Vicente, J. Lanchares, and R. Hermida, Phys. Lett. A **317**, 415 (2003).
[6] Y.-Z. Xu, C. H. Yeung, H.-J. Zhou, and D. Saad, Phys. Rev. Lett. **121**, 210602 (2018).
[7] E. B. Mpemba and D. G. Osborne, Phys. Educ. **4**, 172 (1969).
[8] M. Jeng, Am. J. Phys. **74**, 514 (2006).
[9] A. Gijón, A. Lasanta, and E. R. Hernández, Phys. Rev. E **100**, 032103 (2019).
[10] A. Lasanta, F. Vega Reyes, A. Prados, and A. Santos, Phys. Rev. Lett. **119**, 148001 (2017).
[11] A. Torrente, M. A. López-Castaño, A. Lasanta, F. V. Reyes, A. Prados, and A. Santos, Phys. Rev. E **99**, 060901(R) (2019).
[12] A. Nava and M. Fabrizio, Phys. Rev. B **100**, 125102 (2019).
[13] M. Baity-Jesi, E. Calore, A. Cruz, L. A. Fernandez, J. M. Gil-Narvión, A. Gordillo-Guerrero, D. Iñiguez, A. Lasanta, A. Maiorano, E. Marinari *et al.*, Proc. Natl. Acad. Sci. U.S.A. **116**, 15350 (2019).
[14] I. A. Martínez, A. Petrosyan, D. Guéry-Odelin, E. Trizac, and S. Ciliberto, Nat. Phys. **12**, 843 (2016).
[15] Z. Tu, Phys. Rev. E **89**, 052148 (2014).
[16] O. Abah and E. Lutz, Phys. Rev. E **98**, 032121 (2018).
[17] K. Brandner, K. Saito, and U. Seifert, Phys. Rev. X **5**, 031019 (2015).
[18] O. Raz, Y. Subasi, and R. Pugatch, Phys. Rev. Lett. **116**, 160601 (2016).
[19] Z. Lu and O. Raz, Proc. Natl. Acad. Sci. U.S.A. **114**, 5083 (2017).
[20] M. Bauer, R. Chetrite, K. Ebrahimi-Fard, and F. Patras, Lett. Math. Phys. **103**, 331 (2013).
[21] B. Gaveau and L. Schulman, Phys. Lett. A **229**, 347 (1997).
[22] See Supplemental Material at http://link.aps.org/supplemental/10.1103/PhysRevLett.124.060602 for examples of the precooling strategy in the thermodynamic limit of the antiferromagnet Ising mean-field (nonlinear dynamics) and a Brownian particle, as well as details on the state preparation of the 2D Ising model.
[23] D. E. Kirk, *Optimal Control Theory: An Introduction* (Courier Corporation, New York, 2012).
[24] J. Nocedal and S. Wright, *Numerical Optimization* (Springer Science & Business Media, New York, 2006).
[25] J. Koenemann, G. Licitra, M. Alp, and M. Diehl, Rob. Sci. Syst. (2019).
[26] S. Still, D. A. Sivak, A. J. Bell, and G. E. Crooks, Phys. Rev. Lett. **109**, 120604 (2012).
[27] $p(x, t)$ was calculated using the method presented in Ref. [28].
[28] R. Grima and T. J. Newman, Phys. Rev. E **70**, 036703 (2004).
[29] I. Klich, O. Raz, O. Hirschberg, and M. Vucelja, Phys. Rev. X **9**, 021060 (2019).
[30] We assume that the projection of $\mathbf{v}_2$ into the 2D space is nonzero. If it is zero, then a different set of observables x_1 and x_2 can be chosen.
[31] In the rare cases where the projections of $\mathbf{v}_2$ and $\mathbf{v}_i$ happens to coincide, a different set of observables x_1 and x_2 must be chosen.
[32] R. J. Glauber, J. Math. Phys. (N.Y.) **4**, 294 (1963).